Lamin Proteolysis Facilitates Nuclear Events During Apoptosis

Lakshmi Rao,* Denise Perez,* and Eileen White*‡

*Center for Advanced Biotechnology and Medicine,‡Department of Molecular Biology and Biochemistry, Cancer Institute of New Jersey and Rutgers University, Piscataway, New Jersey 08854

Abstract. Expression of the adenovirus E1A oncogene stimulates both cell proliferation and p53-dependent apoptosis in rodent cells. p53 implements apoptosis in all or in part through transcriptional activation of *bax*, the product of which promotes cell death. The adenovirus E1B 19K product is homologous in sequence and in function to Bcl-2, both of which bind to and inhibit the activity of Bax and thereby suppress apoptosis. The E1B 19K protein also interacts with the nuclear lamins, but the role of this interaction in the regulation of apoptosis is not known. Lamins are, however, substrates for members of the interleukin-1β–converting enzyme (ICE) family of cysteine proteases that are activated during apoptosis and function downstream of Bcl-2 in the cell death pathway. Lamins are degraded during E1A-induced p53-dependent apoptosis. Lamin A and C are cleaved into 47- and 37-kD fragments, respectively, and the site of proteolysis is mapped to a conserved aspartic acid residue at position 230. The cleavage of lamins during apoptosis is consistent with the activation of an ICE-related cysteine protease downstream of p53. No lamin protease activity was detected in cells expressing the E1B 19K protein, indicating that 19K functions upstream of protease activation in inhibiting apoptosis. Substitution of the aspartic acid at the cleavage site produced a mutant lamin protein that was resistant to proteolysis both in vitro and in vivo. Expression of uncleavable mutant lamin A or B attenuated apoptosis, delaying cell death and the associated DNA fragmentation by 12 h. Mutant lamin expressing cells failed to show the signs of chromatin condensation and nuclear shrinkage typical of cell death by apoptosis. Instead, the nuclear envelope collapsed and the nuclear lamina remained intact. However, the late stage of apoptosis was morphologically unaltered and formation of apoptotic bodies was evident. Thus, lamin breakdown by proteolytic degradation facilitates the nuclear events of apoptosis perhaps by facilitating nuclear breakdown.

Apoptosis is a genetically regulated mechanism of cell death commonly observed during development, disease, and viral infections, and is required to maintain homeostasis in multicellular organisms (Raff, 1992; White, 1996). The cellular morphology associated with the apoptotic process has been well documented and is characterized by chromosome condensation, membrane blebbing, formation of apoptotic bodies, and DNA fragmentation (Wyllie, 1980). The molecular mechanisms of apoptosis are just beginning to be understood. Several vertebrate, invertebrate, and viral genes and gene products that regulate apoptosis have been identified (White, 1996).

The regulation of apoptosis during adenovirus infection and transformation has been well studied. The adenovirus E1A oncogene promotes cellular DNA replication (Moran, 1993), which is countered by a cellular response manifested by the induction of p53, accumulation of which causes apoptosis. As a result, productive infection or effective transformation by E1A is impaired (White, 1995; White et al., 1991, 1994). Apoptosis can be overcome by the coexpression of E1A with a second gene product, either the adenovirus E1B 19K protein or the human protooncogene *bcl-2* (Chiou et al., 1994*a*; Rao et al., 1992). E1B 19K is the adenovirus homologue of Bcl-2, as both overcome apoptosis and possess limited amino acid sequence similarity (Chiou et al., 1994*b*).

Apoptosis induced by E1A is p53 dependent, as dominant interfering mutants of p53 can cooperate with E1A to transform primary baby rat kidney (BRK)[1] cells (Debbas and White, 1993). E1A and a temperature-sensitive mutant of p53 (Val135) effectively transform BRK cells at the restrictive temperature of 38°C, but cells rapidly undergo apoptosis when incubated at 32°C (the permissive temperature) when p53 is predominantly wild type. E1B 19K expression completely inhibits the induction of apoptosis by p53 (Debbas and White, 1993). Furthermore, p53-mediated transactivation of the Bax gene product, a death-promoting member of the Bcl-2 family, is one mechanism

Address all correspondence to Eileen White, Center for Advanced Biotechnology and Medicine, 679 Hoes Lane, Piscataway, NJ 08854. Tel.: (908) 235-5329. Fax: (908) 235-5318. e-mail: ewhite@mbcl.rutgers.edu

1. *Abbreviations used in this paper*: BRK, baby rat kidney; GST, glutathione-*S*-transferase; ICE, interleukin-1β–converting enzyme; IL, interleukin; PARP, poly(ADP-ribose) polymerase; TLCK, Tos-Lys-CH_2Cl.

known to be responsible for the onset of apoptosis in these cells (Han et al., 1996*a*). Factors and events downstream of Bax are yet to be elucidated.

Studies in the nematode *Caenorhabditis elegans* have been greatly instrumental in establishing the genetic determinants underlying programmed cell death. Induction of cell death in *C. elegans* is controlled by *ced-3* and *ced-4* (Ellis et al., 1991). The Ced-3 gene product is essential for activating the death program in *C. elegans* (Ellis and Horvitz, 1986), and cloning and sequencing of the gene revealed homology to interleukin-Iβ–converting enzyme (ICE) (Yuan et al., 1993). ICE is a mammalian cysteine protease that recognizes and cleaves prointerleukin (IL)–1β to its active form at aspartate residues (Thornberry et al., 1992). Although overexpression of ICE induces apoptotic events in Rat-1 cells (Miura et al., 1993), ICE-deficient mice develop normally with no defects in apoptosis (Kuida et al., 1995; Li et al., 1995). Numerous mammalian ICE-related proteases whose expression induces apoptosis have since been identified (Fraser and Evan, 1996). These include Nedd-2/ICH-1 (Kumar et al., 1994; Wang et al., 1994), CPP32/Yama/Apopain (Fernandes-Alnemri et al., 1994; Nicholson et al., 1995; Tewari et al., 1995), Tx/ICH-2/$ICE_{rel\text{-}II}$ (Faucheu et al., 1995; Kamens et al., 1995; Munday et al., 1995), $ICE_{rel\text{-}III}$ (Munday et al., 1995), Mch-2 (Fernandes-Alnemri et al., 1995*a*), ICE-LAP3/Mch-3/CMH-1 (Duan et al., 1996; Fernandes-Alnemri et al., 1995*b*), and FLICE/MACH (Boldin et al., 1996; Muzio et al., 1996). Furthermore, the activation of ICE-related proteases is downstream of Bcl-2 in the molecular ordering of the apoptosis pathway (Chinnaiyan et al., 1996). Clearly, ICE-related proteases are an important component of the apoptotic machinery.

Identifying the downstream substrates is the key to understanding the role of these proteases in vivo. The nuclear enzyme poly(ADP-ribose) polymerase (PARP) is a substrate of a protease resembling ICE (prICE) in a cell-free in vitro system (Lazebnik et al., 1994). Both PARP and IL-1β–deficient null mice develop normally with only specific defects in the inflammation process with IL-1β loss (Zheng et al., 1995) and epidermal hyperplasia in the absence of PARP (Wang et al., 1995). This suggests that multiple downstream substrates of the ICE-related cysteine proteases are responsible for bringing about different apoptotic events. Other substrates identified include lamins A, B, and C, the 70-kD protein component of the U1 small ribonucleoprotein, α-fodrin, topoisomerase I, and β-actin, but the role of any of these substrates in apoptosis is not yet clear (Fraser and Evan, 1996; Martin and Green, 1995).

It is attractive to think that proteolytic cleavage of the nuclear lamins by ICE family members plays a role in some of the events associated with apoptosis. The lamins are intermediate filament proteins that constitute the main structural components of the lamina underlying the inner nuclear membrane and serve to organize the chromatin (McKeon, 1991). Lamins A and C are alternatively spliced products of the same gene and differ only in their carboxy terminus. The B-type lamins are distinct but structurally related proteins (Nigg, 1992). Both A- and B-type lamins are characterized by an α-helical rod domain to enable assembly into filaments, a nuclear localization sequence to direct them to the nucleus, and a carboxy-terminal CAAX box isoprenylation sequence for nuclear membrane targeting (McKeon, 1991). Lamin disassembly at the onset of mitosis occurs by hyperphosphorylation at specific sites flanking the α-helical rod domain by $p34^{cdc2}$ kinase (Peter et al., 1990; Ward and Kirschner, 1990). Lamin polymerization is required for nuclear reassembly after mitosis, suggesting that the lamins play an important role in nuclear organization (Heald and McKeon, 1990; Nigg, 1992). However, during apoptosis, lamin disassembly is accomplished through cleavage by a protease related to ICE (Earnshaw, 1995; Lazebnik et al., 1995).

Lamin proteolysis during apoptosis has been reported from several cell types. Etoposide-induced apoptosis in HL-60 cells is accompanied by extensive protein degradation and diminished levels of lamin B (Kaufmann, 1989). Similarly, activation-driven cell death of T cells causes solubilization of the nuclear lamins (Ucker et al., 1992). Lamin degradation is also observed in apoptosis induced by serum starvation of *ras* transformed primary rat embryo cells where lamin A and B are degraded into a 46-kD fragment in parallel with chromatin condensation (Oberhammer et al., 1994). Lamin B1 degradation in apoptotic thymocytes was reported to precede the onset of DNA fragmentation (Neamati et al., 1995). Proteolysis of lamin A into a 45-kD fragment has been demonstrated using cell free extracts in vitro, suggesting that an ICE-like protease is responsible (Lazebnik et al., 1995). Lamin cleavage in vitro is inhibited by protease inhibitors like Tyr-Val-Ala-Asp-CH_2Cl (YVAD-cmk) and Tos-Lys-CH_2Cl (TLCK) (Lazebnik et al., 1995).

The contribution of lamin degradation to cell death by apoptosis remains obscure. We have demonstrated that lamin cleavage occurs during p53-dependent apoptosis, and the site of lamin cleavage was identified as a conserved aspartic acid residue at position 230. Alteration of this aspartic acid to an alanine by site-directed mutagenesis produced a mutant lamin protein that was resistant to proteolysis in vivo and in vitro. Ectopic expression of an uncleavable mutant of lamin A or B caused a significant delay in the onset of apoptosis. Analysis of the ultrastructure and morphology of these cells revealed the requirement of lamin proteolysis in bringing about some of the nuclear events associated with apoptosis. The mutant lamin-expressing cells displayed a delay in nuclear shrinkage and an absence of normal chromatin condensation. Instead, the nuclei collapsed in on themselves while retaining an intact lamina and nuclear envelope. However, the late stages of apoptosis are similar to the parental cells as seen by the formation of apoptotic bodies. Thus, proteolytic cleavage of lamins in vivo is required for normal progression of apoptotic cell death.

Materials and Methods

Cloning and Plasmid Constructions

The lamin A cDNA was reverse transcription–PCR cloned using RNA from Hela cells as the template. Specific primers incorporating BstXI and NotI sites were used at the 5′ and 3′ end, respectively, to include initiation and termination sites. The cDNA was cloned into the BstXI/NotI sites of the pRcCMV vector (Invitrogen, San Diego, CA). The lamin B cDNA (Pollard et al., 1990) was obtained in the pBLUESCRIPT vector from Dr.

Michael Pollard (Research Institute of Scripps Clinic, La Jolla, CA). The sequence of these constructs was verified, and they were used as templates for all subsequent cloning and mutation steps.

Glutathione-*S*-transferase (GST) fusion protein of a fragment of lamin A (GST LA220-390) was constructed by PCR cloning from the full-length lamin A template using specific primers with EcoRI and XhoI sites engineered to clone in frame with the GST protein in the pGEX4T-1 vector (Pharmacia Fine Chemicals, Piscataway, NJ). The primers used were: LA_{220}- ATTCTTGAATTCGCGCCGTCATGAGACCCGA and LA_{390}r-ATTATTCTCGAGGGACAGGCGTAGCCTCTC. GST LB220-390 was constructed by the same strategy into the EcoRI/XhoI sites of the pGEX4T-1 vector. The primers used were: LB_{220}- ATTCTTGAATTCAGGAAGCATGAAACGCGC and LB_{390}r- ATTATTCTCGAGCAGCTTCAACCTCTCTTC. The D → A mutation was created using a long oligonucleotide at the 5′ end to make a single base substitution and to incorporate the amino acid change. This was used in conjunction with the 3′ oligonucleotide listed above to prime the synthesis of a PCR product that was cloned into the EcoRI/XhoI sites of the pGEX4T-1 vector. The primers used were: LA_{220} mut- ATTCTTGAATTCGCGCCGTCATGAGACCCGACTGGTGGAGATTGCCAAT and LB_{220} mut-ATTCTTGAATTCAGGAAGCATGAAACGCGCTTGGTAGAGGTGGCT.

The full-length lamin A and lamin B mutants were constructed with the same basic strategy. A unique restriction site (BspHI) was identified within 40 bases of the aspartate residue to be changed to alanine. Oligonucleotides were designed from the ATG of the gene including an XmaI site upstream to be in frame with a myc or FLAG epitope tag. The primer at the 3′ end included the termination site followed by an XhoI site. Internal primers had a single base substitution to incorporate the amino acid change from aspartate to alanine. PCR was performed to generate two fragments of each gene that were ligated at the unique BspHI site to regenerate the full-length product. The full-length lamin A and lamin B cDNAs containing the single base substitution were cloned into the KpnI/XhoI sites of pCEP4 and pcDNA3 (Invitrogen) vectors, respectively. The myc tag has been previously reported (Han et al., 1996*a*), and the FLAG tag amino acid sequence corresponded to DYKDDDDK. Standard PCR conditions and protocols were used in all cases. The constructs were verified for sequence and presence of the mutation confirmed by using an automated sequencer (ABI 373; Perkin-Elmer Corp., Foster City, CA).

Cell Lines, Transfections, and Viability and DNA Fragmentation Assays

An1, 19K1, 19K2, p53A, and 4P cell lines have been previously described (Debbas and White, 1993). The E1A plus p53 (Val135) transformed BRK line p53A was transfected by electroporation with a hygromycin-resistant vector (pCEP4) or a corresponding mutant lamin A–carrying plasmid (pCEP4-LA mut). Transformants were screened by Western blotting using an anti-myc epitope antibody. Three independent clones (LA-1, LA-2, and LA-3) and two vector controls (Vh1 and Vh2) were derived and maintained at 38°C. LA-1, LA-2, and Vh1 were then transfected with a neo vector (pcDNA3) or a plasmid carrying mutant lamin B with a FLAG epitope tag (pcDNA3-LB mut). Cell lines expressing neither protein, either lamin A or lamin B, and both lamin A and lamin B were screened as described above using anti-myc and -FLAG mAbs by Western blotting. All cell lines were maintained in DME with 5% FBS and maintained at 38°C (restrictive temperature) unless otherwise mentioned. Viability assessments were made by trypan blue exclusion as described previously (Chiou et al., 1994*a*). Low molecular weight DNA was extracted from the vector control cell line and two representative mutant lamin-expressing cell lines after incubating at 38°C (0 h) and at 32°C for 8, 16, 24, and 48 h by the method of Hirt (1967) with minor modifications (White et al., 1984). Equal volumes of the Hirt supernatant were resolved on a 1% agarose gel, and degraded DNA was visualized by staining with ethidium bromide.

Western Blotting and Antibodies

Extracts were obtained from subconfluent cultures, and the protein concentration was determined. 40 μg of each protein sample was subjected to SDS-PAGE and semidry blotted onto nitrocellulose membranes. Subsequent to incubation with appropriate primary and secondary antibodies, immune complexes were detected by enhanced chemiluminescence according to the manufacturer's instructions (ECL; Amersham Corp., Arlington Heights, IL). The lamin A/C antibodies (McKeon et al., 1988) were a kind gift of Dr. Frank McKeon (Harvard Medical School, Boston, MA), and the murine anti-p53 antibody (pAb248) was generously provided by Dr. Arnold Levine (Princeton University, Princeton, NJ). Antibodies directed to lamin B (Matritech, Inc., Cambridge, MA), the myc epitope (Calbiochem-Novabiochem Corp., La Jolla, CA), the FLAG epitope (Scientific Imaging Systems, New Haven, CT), E1A (M73) (Calbiochem-Novabiochem Corp.), GST (Santa Cruz Biotechnology, Santa Cruz, CA), PARP (C-2-10) (Enzyme Systems Products, Dublin, CA), and actin (Amersham Corp.) were purchased and used according to the manufacturer's specifications.

In vitro Proteolysis Assay

Cytosolic extracts of the cells to be assayed for protease activation were prepared as described (Nicholson et al., 1995). In brief, cells at 38°C (0 h, nonapoptotic) or after incubation at 32°C (apoptotic) were harvested with medium and washed with PBS. All cells were counted and resuspended in ice-cold lysis buffer containing 10 mM Hepes, 2 mM EDTA, 0.1% CHAPS, 5 mM DTT, 1 mM PMSF, 20 μg/ml leupeptin, 10 μg/ml pepstatin A, and 10 μg/ml aprotinin at 10^8 cells per ml. Lysates were repeatedly spun at 12,000 *g* for 10 min to remove cellular debris, and aliquots of the supernatant were stored under liquid nitrogen. To assess the kinetics of lamin cleavage in the time-course experiments, the extracts were equalized for protein concentration.

GST LA220-390, GST LB220-390, and their respective D → A mutants were purified from BL21 *Escherichia coli* after induction with isopropyl-thio-β-D-galactoside. Purification was achieved on glutathione–Sepharose according to the manufacturer's instructions (Pharmacia Fine Chemicals). Purified protein was eluted from the beads and quantitated. Cytosolic extracts were mixed with purified proteins at a concentration of 0.5 μg protein per 10 μl of extract and incubated at 37°C. The reactions were stopped by the addition of Laemmli sample buffer and boiling. An aliquot taken before incubation represented the 0-h time point. Samples were resolved on SDS-PAGE gels, transferred to nitrocellulose membranes, and blotted using anti-GST antibodies as described above.

Ultrastructural Analysis

Samples for EM were obtained from a mutant lamin A and B–expressing cell line (LA1-LB1) and a corresponding vector control line (Vh1-n1) at 38°C and after 24 h at 32°C. Cells were processed, viewed, and photographed as previously described (Rao et al., 1992).

Indirect Immunofluorescence

Cells were plated at low density onto glass coverslips. The cells, incubated either at 38°C or 32°C, were fixed and processed for indirect immunofluorescence as described previously (White and Cipriani, 1989). Endogenous lamin A/C, the myc epitope–tagged mutant lamin A, or the FLAG epitope–tagged mutant lamin B were visualized using the primary antibodies described earlier and a rhodamine-conjugated anti–mouse secondary antibody (Jackson ImmunoResearch Laboratories, Inc., West Grove, PA). The cells were simultaneously stained with Hoechst dye for DNA. The terminal phenotype of the cells was assessed by labeling with Hoechst dye in vivo and harvesting the floating cells in the medium after 28 h at 32°C. The cells were then washed with PBS and visualized by wet mounting onto slides. All slides were examined and photographed by a microscope with epifluorescence optics (FXA; Nikon Inc., Garden City, NY).

Results

Degradation of Nuclear Lamins during p53-dependent Apoptosis

Induction of apoptosis by adenovirus E1A has been previously characterized and shown to be mediated by wild-type p53 (Chiou et al., 1994*a*; Debbas and White, 1993; Sabbatini et al., 1995*a*, *b*). Primary BRK cells transformed by E1A and temperature-sensitive p53 (Val135) proliferate at the restrictive temperature of 38°C but undergo apoptosis at the permissive temperature of 32°C when p53 is predominantly in the wild-type conformation (Debbas and

White, 1993). Transcriptional activation of the death-promoting protein Bax by p53 is one mechanism for the induction of apoptosis in these cells (Han et al., 1996*a*). Events downstream of Bax are poorly understood. To understand the role of cysteine proteases, if any, we investigated the status of nuclear lamins in these cells. Proteolysis of lamins has been reported from a variety of systems, and lamins represent a ubiquitous substrate of proteases activated during apoptosis (Earnshaw, 1995). We evaluated whether lamin proteolysis occurred during p53-dependent apoptosis.

An1 is a BRK cell line transformed with E1A and temperature-sensitive p53 (Val135). These cells proliferate at the restrictive temperature of 38°C but undergo apoptosis at the permissive temperature of 32°C when p53 is wild type. 19K1 and 19K2 are identical E1A plus p53 (Val135) transformed BRK cell lines that stably express the E1B 19K protein and thus are protected from apoptosis. 4P, a BRK line transformed with E1A and E1B, serves as a control. Lamins A and C are essentially identical except for their carboxy termini. Both proteins are recognized by a COOH-terminal mAb and seen as 73- and 63-kD proteins, respectively (Fig. 1).

Western blot analysis of extracts from cells undergoing p53-dependent apoptosis revealed the degradation of the nuclear lamins with increasing time at the permissive temperature when p53 is wild type (Fig. 1). An1 cells began to show morphological signs of apoptosis between 12 and 16 h of incubation at 32°C (data not shown). Degradation products of lamin A and C were seen as two discrete bands of ~47 and 37 kD, respectively, and appeared ~10 h after incubation at 32°C. These results are consistent with findings published previously and indicate a cleavage site near the center of the lamin A protein. Lamin B degradation products were not as evident since the levels of lamin B in BRK cells were low (Fig. 1). There was no obvious degradation of lamin A, B, or C in the cells expressing the E1B 19K protein where apoptosis was inhibited (Fig. 1). Furthermore, lamin degradation was observed before nonspecific proteolysis of E1A and murine p53 occurring in An1 cells after 24 and 48 h of incubation at 32°C, at which point overall cellular degradation occurred.

After 24 h at 32°C, morphological changes associated with late stage apoptosis typified by chromatin condensation was observed (Fig. 2). Concomitantly, staining the same cells with the lamin A/C antibody showed disappearance of the lamina and was consistent with lamin degradation (Fig. 2). E1B 19K–expressing cells incubated at 32°C showed no obvious changes in morphology or lamin staining when compared with the cells incubated at 38°C (Fig. 2).

Mapping of the Lamin Cleavage Site

The ICE family of cysteine proteases is activated upon various forms of stimuli resulting in the induction of apoptosis. These proteases recognize and cleave at a conserved aspartic acid residue in the P1 position of a consensus cleavage site in all known substrates. This is in the context of other flanking amino acids, which possibly lends specificity (Martin and Green, 1995). PARP, a substrate of var-

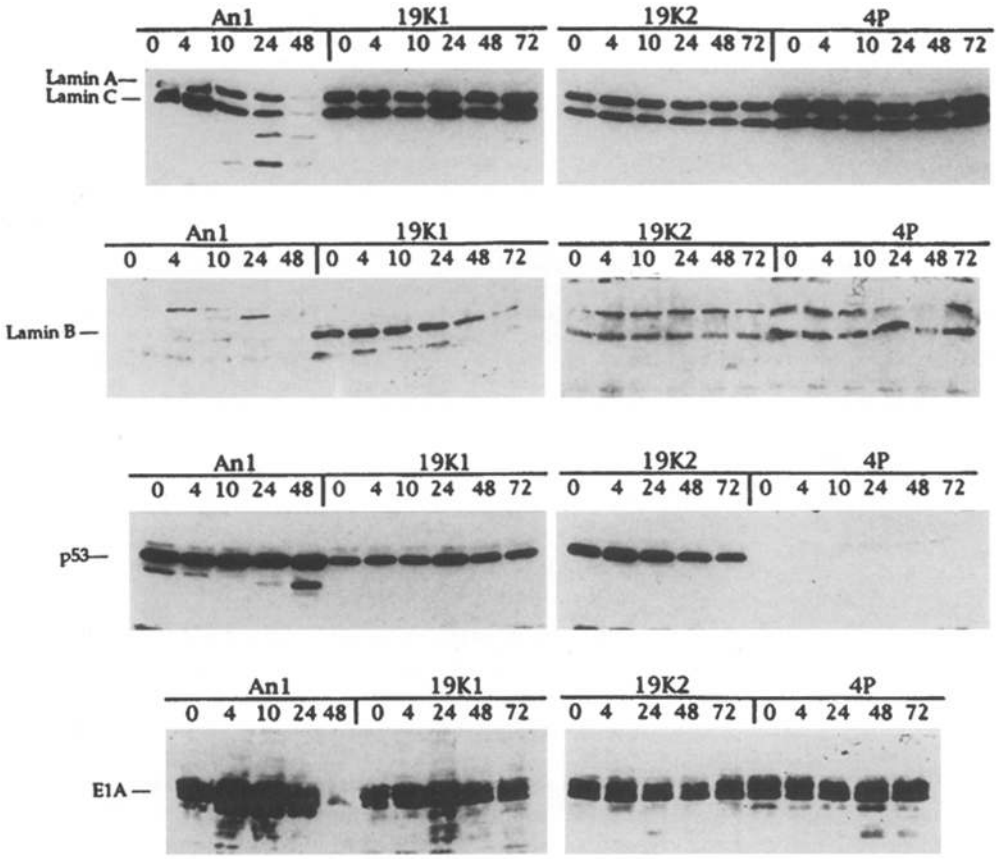

Figure 1. Lamins are degraded during E1A-induced p53-dependent apoptosis. Western blot analysis of lamin degradation in An1, 19K1, 19K2, and 4P cell lines at the restrictive and permissive temperatures. Total cell extracts were prepared from An1 cells at the restrictive temperature (0 h) and after incubation for 4, 10, 24, and 48 h at the permissive temperature. Extracts for the 19K1, 19K2, and 4P lines were prepared at the restrictive temperature and after incubation for 4, 10, 24, 48, and 72 h at the permissive temperature. Western blots were probed with antibodies specific for lamin A/C, lamin B, murine p53 (pAb 248), and E1A (M73).

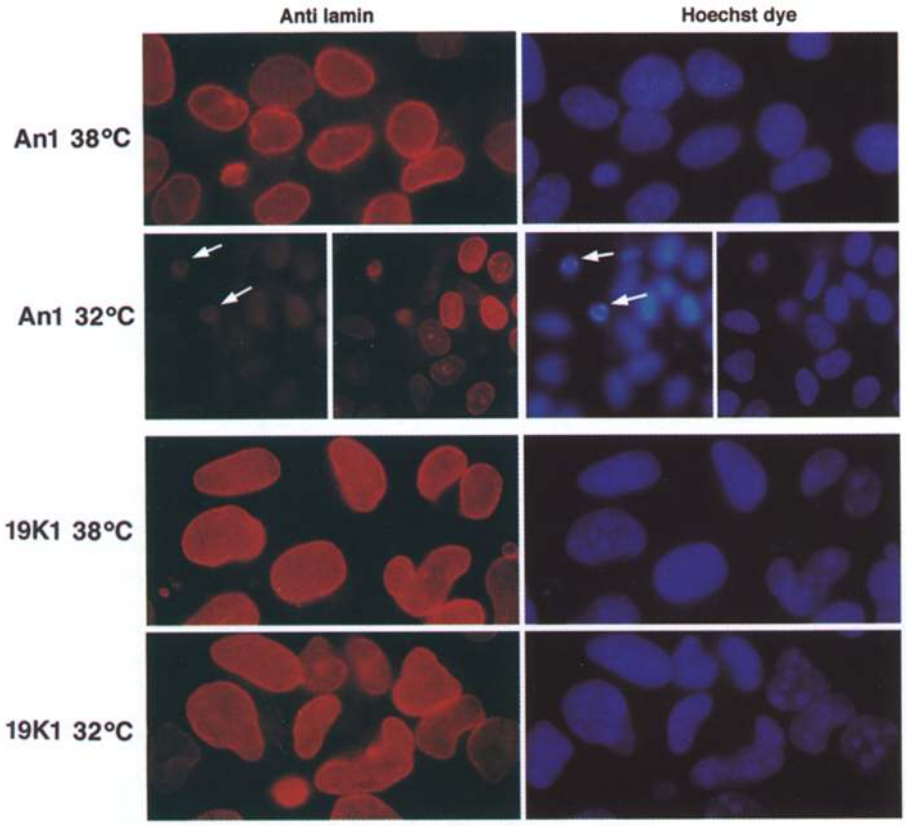

Figure 2. In vivo evidence for disappearing lamina during p53-dependent apoptosis. An1 and 19K1 cells were stained by indirect immunofluorescence for lamin A/C and by Hoechst dye for DNA at 38°C (restrictive temperature) or after 24 h at 32°C (permissive temperature). An1 cells at 32°C were photographed in two planes of focus to clearly show the cells undergoing apoptosis as evidenced by chromatin condensation (*arrows*).

ious cysteine proteases activated during apoptosis, is cleaved at an aspartate in the context of its cleavage site DEVD⇓G (Lazebnik et al., 1994; Nicholson et al., 1995). Lamin A contains two putative cleavage consensus sites, the aspartic acid residues at position 230 and 446 in the context of EVDNG and EIDSG, respectively. However, the appearance of 47- and 37-kD bands in the Western blot (Fig. 1) corresponding to lamin A and C using a COOH-terminal antibody indicated the presence of a single cleavage site consistent with that at Asp230. Furthermore, this aspartate is conserved among lamins from human, mouse, chicken, *Xenopus*, and *Drosophila* as also lamin B and vimentin (Fig. 3 *a*). To test if Asp230 was indeed a valid cleavage site recognized by a cysteine protease, we devised an in vitro cleavage assay.

Fragments of human lamin A/C and lamin B from amino acids 220–390 (which included the putative cleavage site) were generated as fusion proteins with GST (GST LA220-390 and GST LB220-390) (Fig. 3 *b*). These fusion proteins were purified over glutathione-Sepharose beads. When cleaved at the consensus site, a GST protein product of ~27 kD would be generated, which could be conveniently assayed by Western blotting with an anti-GST antibody. A corresponding substitution mutation resulting in the change of the P1 aspartate to alanine was also generated (GST LA220-390 D→A mutant and GST LB220-390 D→A mutant) (Fig. 3 *b*). If the site were recognized by a cysteine protease, the change would render the D→A mutant resistant to cleavage. Cytoplasmic extracts from E1A plus p53 (Val135) transformed cells at 38°C (nonapoptotic) and after 14 h at 32°C (apoptotic) were used to assay for protease activity. The lamin fragment–GST fusion proteins described above were incubated with these extracts at 37°C for increasing lengths of time and Western blotted using an anti-GST antibody to detect cleavage products, if any. As seen in Fig. 4, *a* and *c*, protease activity was detected in the cytoplasmic extracts of apoptotic cells with the capacity to cleave the GST–lamin fusion proteins and generated a cleavage product corresponding to the expected size of ~27 kD migrating with GST alone. An increase in the amount of cleavage product formed was observed with increasing time, consistent with an enzymatic activity. Furthermore, the D→A mutant of the same protein was resistant to cleavage, confirming the site of proteolysis to be VEID⇓N for lamin A and VEVD⇓S for lamin B.

Activation of ICE-related Proteases during Apoptosis and Inhibition of Activation by E1B 19K Expression

The lamin cleavage activity appeared in the apoptotic 32°C extract but not in the nonapoptotic 38°C extract of An1 cells, suggesting that protease activation lies downstream of p53 (Fig. 4, *a* and *c*). No protease activity was detected in extracts from cells stably expressing the E1B 19K protein incubated either at 38° or 32°C (Fig. 4, *b* and *d*). The E1B 19K protein expression also prevents the processing of CPP32 and cleavage of PARP in CHO cells infected with adenoviruses (Boulakia et al., 1996). The absence of lamin cleavage activity in E1B 19K–expressing cells observed here further reinforces the role of the E1B 19K protein as an inhibitor of apoptosis and places it upstream of protease activation in the apoptotic pathway.

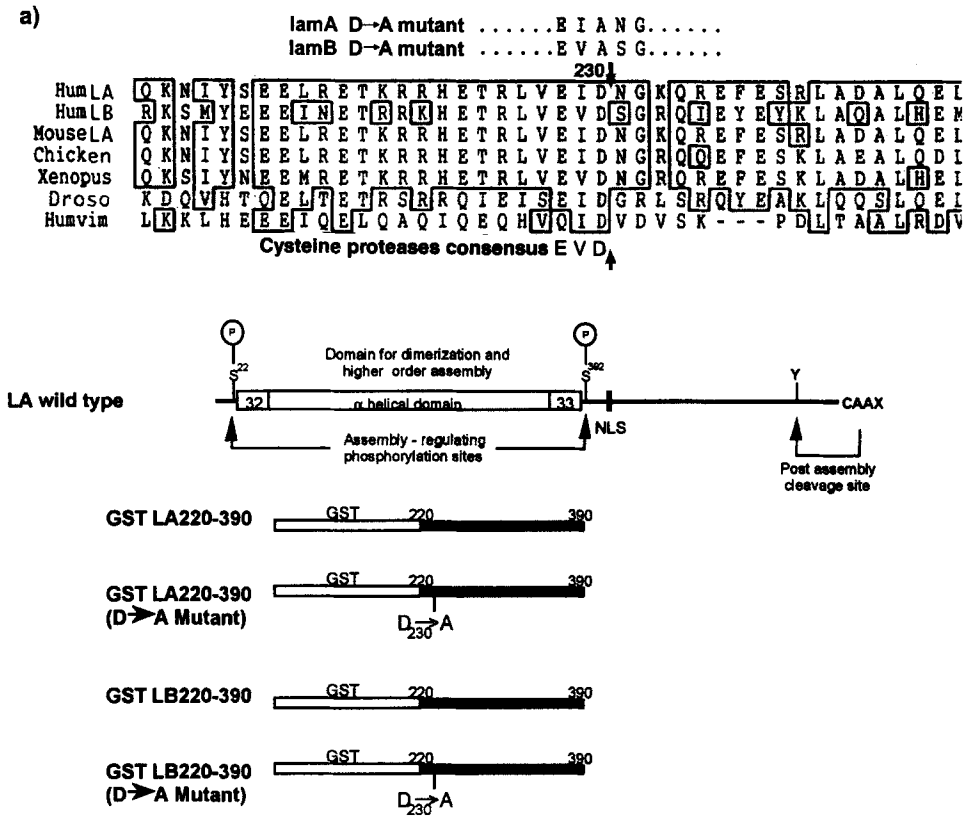

Figure 3. Location of lamin cleavage sites and cleavage site mutants. (*a*) Amino acid sequence alignment of lamins from different species and human vimentin from amino acids 207–248 that includes the putative cleavage site. The aspartate at position 230 is marked by an arrow and constitutes the site of cleavage. The mutations used to change this aspartate are indicated. (*b*) Main structural features of lamin A are indicated. Schematic representation of the GST constructs used to generate fragments of lamins and their mutants to assay for in vitro cleavage and protease activity. Open regions correspond to GST sequences in the fusion protein, and the lamin sequences are indicated by closed boxes. The exact location of the mutation is represented.

Kinetics of the Activation of Lamin Proteases during p53-dependent Apoptosis

The temperature-sensitive p53 (Val135) protein is cytoplasmic when in the mutant conformation at the restrictive temperature and translocates to the nucleus at the permissive temperature when p53 assumes the wild-type conformation (Martinez et al., 1991; Michalovitz et al., 1990). In the E1A plus p53 (Val135) transformed BRK cells, this process occurs within 3–4 h of incubating the cells at 32°C along with transcriptional induction of the p53-responsive genes *p21/waf-1/cip1* and *Bax* (Han et al., 1996*a*; Sabbatini et al., 1995*b*). However, the morphological changes and loss of viability associated with apoptosis began at ~12 h after incubating the cells at 32°C (data not shown). In understanding the kinetics of events before the final execution of apoptosis, biochemical processes downstream of Bax induction may be important. Using the in vitro lamin proteolysis assay, we sought to determine the kinetics of lamin cleavage and thereby the kinetics of ICE-like cysteine protease activation during p53-dependent apoptosis.

Activation of lamin proteases was assessed in cytoplasmic extracts obtained from An1 and 19K1 cell lines. Extracts were made from cells incubated at either the restrictive temperature or for increasing times at the permissive temperature and were equalized for protein concentration. These extracts were incubated with GST-LA220-390 and GST-LA220-390 (D→A mutant) for 1 h at 37°C and Western blotted with an anti-GST antibody to detect cleavage products. Protease activity was detected at 8 h after incubation at 32°C, as seen by the cleavage product at ~27 kD (Fig. 5 *a*). Peak activity was observed after 12 h at the permissive temperature with no detectable activity remaining by 24 h. The loss of lamin protease activity at 24 h was likely due to the extensive cell death and thereby cell degeneration that had occurred by that time (Fig. 5 *a*). As expected, no lamin cleavage activity was observed when the cleavage site Asp230 (D→A) mutant was used as the substrate (Fig. 5 *a*). Once again, E1B 19K–expressing cells showed no detectable lamin protease activity at any time of incubation at the permissive temperature (Fig. 5 *b*). These results indicate that lamin protease activation was downstream of p53 and possibly occurred as a direct or indirect consequence of Bax induction. The E1B 19K protein inhibits lamin protease activation by acting upstream, likely through interaction with and functional antagonism of Bax. Thus, both the in vivo and in vitro lamin cleavage results suggest that in the time line of events leading to the final execution of the apoptotic program, lamin proteolysis is a significantly early step occurring before nuclear breakdown and loss of cell viability.

Prevention of Lamin Cleavage Attenuates Apoptosis In Vivo

Having characterized the activity of a lamin cleaving protease during p53-dependent apoptosis and the site of cleavage in vitro, we sought to address the significance of lamins as substrates in vivo. The critical role of nuclear events during apoptosis is well established (Earnshaw, 1995). Even though the nuclear envelope remains intact, the chromatin of cells undergoing apoptosis condenses, collapsing against the nuclear periphery, and subsequently buds off into smaller apoptotic bodies (Wyllie, 1980). This

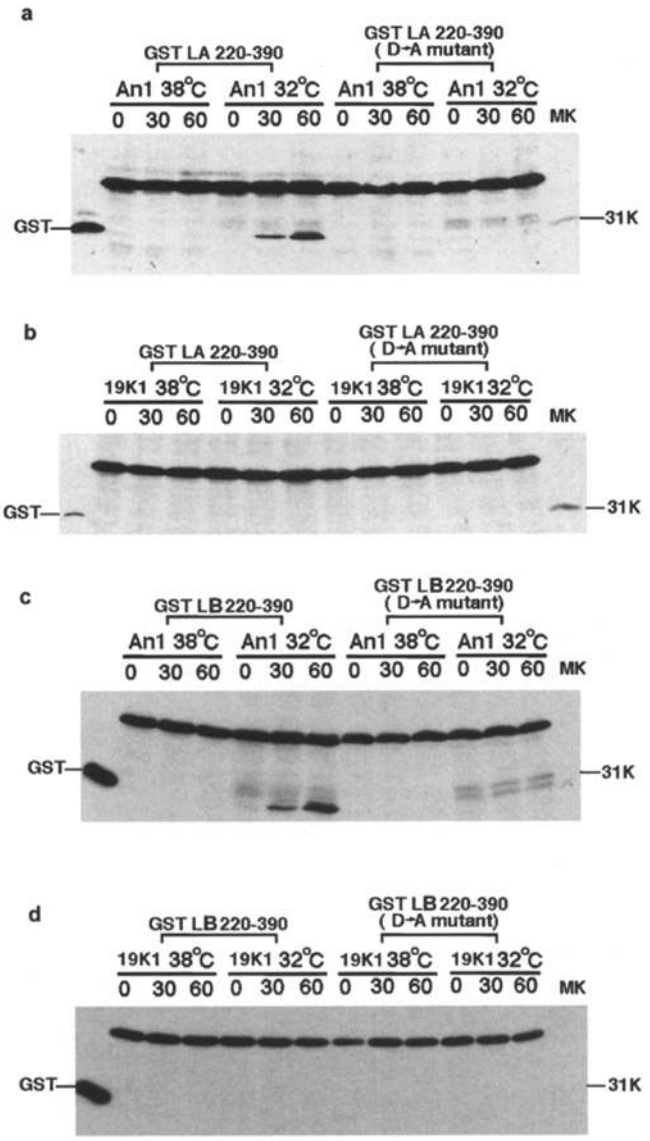

Figure 4. In vitro lamin protease activation during p53-dependent apoptosis, and inhibition by E1B 19K expression. Western blot of GST–mini lamin fusion proteins with an anti-GST antibody. (*a* and *c*) Extracts of An1 cells at 38°C (restrictive temperature, nonapoptotic) and 32°C (permissive temperature, apoptotic) were incubated with GST LA 220-390, GST LB 220-390, and their respective D→A mutants for 0, 30, and 60 min and Western blotted with anti-GST antibodies. The cleavage product comigrates with the GST protein. (*b* and *d*) Cytoplasmic extracts from E1B 19K–expressing cells (19K1) at 38° and 32°C were incubated with the GST–mini lamin fusion proteins and their mutants for 0, 30, and 60 min before Western blotting with anti-GST antibodies. The position of the 31-kD marker is indicated in all blots.

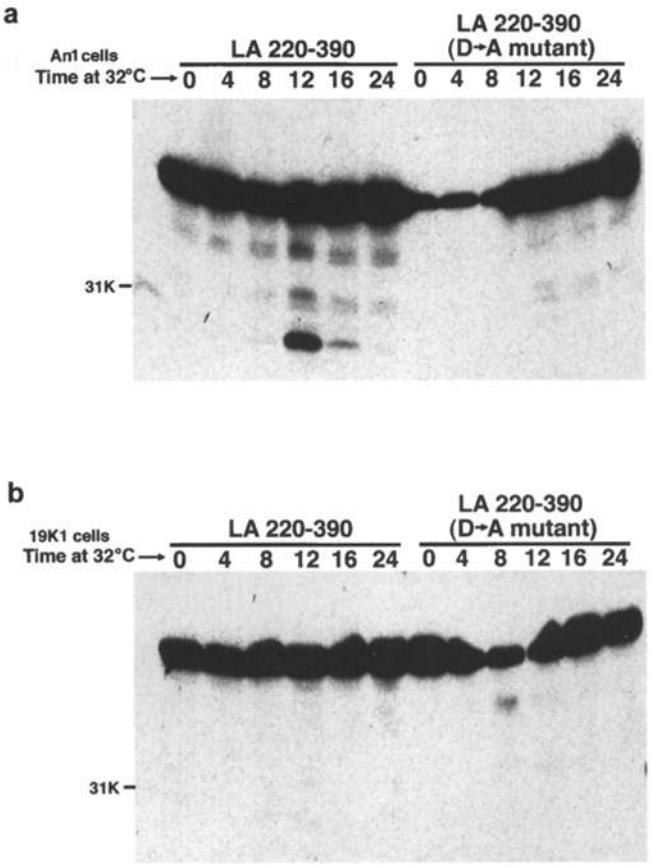

Figure 5. Kinetics of the activation of lamin proteases during p53-dependent apoptosis. (*a*) Extracts from An1 cells at the restrictive temperature (0 h) and after 4, 8, 12, 16, and 24 h at the permissive temperature were incubated with the GST LA 220-390 and GST LA 220-390 (D→A) fusion proteins for 1 h and Western blotted with anti-GST antibodies. The 31-kD marker is shown. (*b*) Extracts from E1B 19K–expressing cells at the restrictive temperature (0 h) and after 4, 8, 12, 16, and 24 h at the permissive temperature were incubated with the fusion proteins for 1 h before Western blotting with anti-GST antibodies. Generation of the lamin cleavage product is indicated by the presence of the 27-kD band.

is an unmistakable hallmark of apoptosis observed in a variety of systems. Inhibition of lamin proteolysis in vitro by the addition of the protease inhibitor TLCK resulted in the arrest of the nuclear changes at the condensed chromatin stage, with the chromatin forming a continuous rim around the nuclear envelope (Lazebnik et al., 1995). However, TLCK is a nonspecific protease inhibitor and likely inhibits more than merely lamin cleavage in a cell-free system.

The cleavage site mutant of human lamin A was reconstituted into the full-length lamin A protein and expressed under the control of a cytomegalovirus promoter. A myc epitope tag allowed the recombinant, uncleavable lamin A to be distinguished from the endogenous lamin A, and a hygromycin drug resistance marker allowed for the selection of stable cell lines. Three cell lines were derived from the parental E1A plus p53 (Val135) transformed cell line, p53A. The myc-tagged mutant lamin A protein was detected in cell lines LA-1, LA-2, and LA-3 by Western blot analysis (Fig. 6 *a*). Vh1 and Vh2 are equivalent vector control cell lines selected at the same time by transfecting the p53A cell line with an empty hygromycin vector (pCEP4). The mutant lamin A in all three cell lines localized to the nuclear periphery and was indistinguishable from endogenous lamin A in proliferating cells at 38°C (see below). Mutant lamin A expression did not alter the rate of cell proliferation, and lamin disassembly was observed in cells undergoing mitosis (data not shown), indicating that lamin

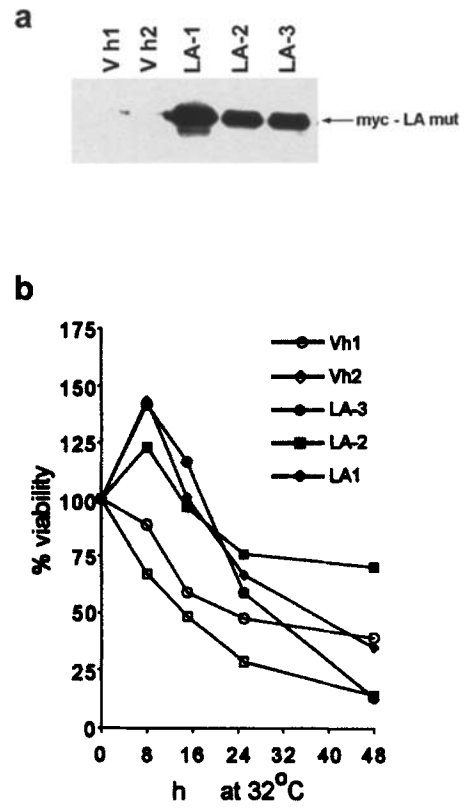

Figure 6. Effect of the expression of mutant lamin A in vivo. (*a*) Levels of expression of mutant lamin A. Three independent clones were selected to express mutant lamin A as seen by the Western blot using anti-myc epitope antibody. Vh1 and Vh2 are vector control lines selected at the same time for hygromycin resistance. (*b*) Viability of the mutant lamin A–expressing cells after 8, 16, 24, and 48 h at 32°C expressed as a percentage of the viability at 38°C (0 h).

cleavage is not involved in the regulation of cell growth or cell cycle control. The mutant lamin A–expressing and the control cell lines were incubated at 32°C and followed for changes in viability. Fig. 6 *b* shows the percentage viability as a function of the time at 32°C. Where the two vector control cell lines lost viability rapidly at 32°C as previously observed for similarly constructed cell lines (Chiou et al., 1994*a*; Debbas and White, 1993; Sabbatini et al., 1995*b*), the three independent mutant lamin A–expressing cell lines displayed delayed onset of viability loss, surviving for an additional 12–16 h at 32°C, and instead the viable cell number increased (Fig. 6 *b*). The kinetics of the morphological signs associated with apoptosis were delayed for 12 h in the mutant lamin A–expressing cells. After 12–16 h at the permissive temperature, however, the mutant lamin A–expressing cells rapidly lost viability and ultimately reached the levels of cell death of the vector control lines by 48 h (Fig. 6 *b*).

While lamin A/C are encoded by the same gene and differ only in their COOH terminus as a result of alternative splicing, lamin B is a distinct but structurally related polypeptide. Lamin B is expressed early in development and in virtually all somatic cell types (Nigg, 1992). We expressed the uncleavable mutant of lamin B in cells to see if the attenuation of apoptosis observed with mutant lamin A could also be achieved by preventing lamin B cleavage, and to determine if preventing cleavage of both lamin A and B could further augment survival. As with the uncleavable lamin A, the cleavage site mutation of human lamin B was reconstituted into the full-length lamin B protein, and a FLAG epitope tag was placed at the NH_2 terminus to distinguish it from both the endogenous lamins and the uncleavable lamin A. The mutant lamin B was expressed by the cytomegalovirus promoter in a vector with a neomycin selectable marker. This allowed for selection of mutant lamin B–expressing clones independent of mutant lamin A, which was introduced by hygromycin selection. Mutant lamin B was transfected into a vector line (Vh1) and two mutant lamin A–expressing clones (LA-1 and LA-2). As the Western blot in Fig. 7 *a* shows, equivalent cell lines were selected to express either mutant lamin A (LA1-n and LA2-n), mutant lamin B (Vh1-LB1 and Vh1-LB2), or both mutants (LA1-LB1, LA1-LB2 and LA2-LB3). These cell lines expressed the mutant lamin proteins at levels comparable to the level of endogenous lamins as detected with anti-myc and -FLAG antibodies (Fig. 7 *a*) or with an anti-lamin mAb (see Fig. 9). The cell lines were incubated at 32°C and assessed for the ability of the mutant proteins to affect p53-dependent apoptosis.

Fig. 7, *b* and *c*, shows the percentage of viability as a function of time for the cell lines expressing mutant lamin A or mutant lamin B, or both mutant lamin A and mutant lamin B, and the corresponding control cell lines. The 19K1 line, which is completely inhibited from cell death as a result of E1B 19K expression, serves as a positive control (Debbas and White, 1993). Expression of either mutant lamin A or mutant lamin B produced a delay in the induction of apoptosis by 12–16 h (Fig. 7 *b*), similar to what was observed previously with the mutant lamin A–expressing cell lines (Fig. 6 *b*). Mutant lamin A expression appeared to be more effective at delaying apoptosis than mutant lamin B expression (Fig. 7 *b*). Expression of both mutant lamin A and lamin B in the same cell was not additive. Viability of the cell lines expressing both mutant lamin A and lamin B (LA1-LB1, LA1-LB2, and LA2-LB3) followed the same course as with cell lines expressing either mutant lamin A or lamin B alone (LA1-n, LA2-n, Vh1-LB1, and Vh1-LB2), and cell death was attenuated by 12–16 h (Fig. 7 *c*). The vector control lines (Vh1-n1 and Vh1-n2) (Fig. 7, *b* and *c*) gradually lost viability, and the cytopathic effects associated with apoptosis were evident after 12 h at 32°C (data not shown). E1B 19K expression in the 19K1 cell line completely overcame apoptosis, and the cells were diverted to p53-dependent growth arrest (Fig. 7 *c*) as previously reported (Sabbatini et al., 1995*a*). The limited protection afforded by uncleavable lamins does not seem to depend on increased protein expression, since no correlation was observed between levels of expression of the mutant proteins and attenuation of apoptosis (Fig. 7; data for other clones not shown). The overall effect, demonstrated with eight independent cell lines expressing uncleavable mutants of the nuclear lamins, was to delay the onset of cell death. Thus, lamin cleavage facilitates the apoptotic process, perhaps by promoting nuclear destruction.

Similar results were observed when the same panel of

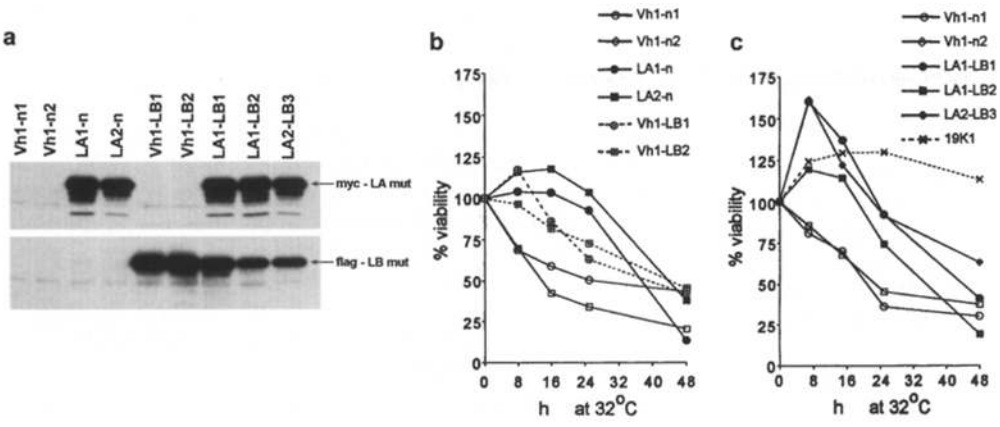

Figure 7. In vivo ectopic expression of the cleavage site mutants of lamin A and lamin B attenuates the induction of p53-dependent apoptosis. (*a*) Selection of cell lines for mutant lamin B expression. Western blot shows independent cell lines selected to express neither mutant lamin protein, mutant lamin A or lamin B, or both mutant lamin A and lamin B. Blots were probed with anti-myc and -FLAG epitope antibodies for detecting mutant lamin A and mutant lamin B, respectively. (*b*) Viability of the cell lines expressing only mutant lamin A or lamin B (*LA1-n*, *LA3-n*, *Vh1-LB1*, and *Vh1-LB2*) after 8, 16, 24, and 48 h at 32°C expressed as a percentage of the viability at 38°C (0 h). (*c*) Viability of the cell lines expressing both mutant lamin A and lamin B (*LA1-LB1*, *LA1-LB2*, and *LA2-LB3*) at 8, 16, 24, and 48 h after incubating at 32°C expressed as a percentage of the viability at 38°C (0 h). 19K1 is an E1B 19K–expressing cell line that is resistant to apoptosis (Debbas and White, 1993). The vector controls in all viability graphs are represented by open boxes and circles.

cell lines was induced to undergo apoptosis by treatment with actinomycin D (data not shown). Actinomycin D induces a p53-independent pathway, as apoptosis is efficiently induced when the cells are maintained at the restrictive temperature of 38°C (Sabbatini et al., 1995*a*). Therefore, preventing the proteolytic degradation of the nuclear lamina by ICE-related cysteine proteases affords significant but limited protection from apoptosis induced by two independent means.

Onset of DNA Fragmentation Is Dependent on Lamin Cleavage In Vivo

Activation of nucleases is a downstream nuclear event during apoptosis as evidenced from oligonucleosomal cleavage of DNA characteristic of apoptosis (Earnshaw, 1995). DNA fragmentation accompanies loss of viability during E1A-induced p53-dependent apoptosis (Debbas and White, 1993). The degradation of lamin B1 in apoptotic thymocytes precedes DNA fragmentation (Neamati et al., 1995), and inhibition of lamin proteases by TLCK does not prevent internucleosomal cleavage of DNA (Lazebnik et al., 1995). These observations suggest that the activation of nucleases is independent of the proteases during apoptosis.

The delay in the onset of apoptosis observed in mutant lamin–expressing cells indicated a role in bringing about the downstream nuclear events of apoptosis. Low molecular weight DNA was isolated from a vector control cell line (Vh1-n2) and two representative mutant lamin–expressing cell lines (LA1-LB1 and LA1-LB3) incubated at 32°C (0 h) and for 8, 16, 24, and 48 h at 32°C. After 8 h at 32°C, coincident with viability loss, cleavage of DNA into oligonucleosomal-size fragments was observed in the vector control cell line (Fig. 8). The time course of DNA fragmentation in the mutant lamin–expressing cell line followed the delay in the loss of viability observed earlier, with no DNA degradation at 8 h and progressively increasing at 16 and 24 h and reflecting the vector control levels by 48 h (Fig. 8). The DNA fragmentation pattern closely followed viability loss in both the vector control and the mutant lamin–expressing cell lines (Figs. 7 *c* and 8). These results suggest a function for lamin proteolysis in facilitating the activation of the nucleases responsible for DNA fragmen-

Figure 8. Delay in the induction of DNA fragmentation in the mutant lamin–expressing cells. Integrity of DNA was determined in a vector control cell line (*Vh1-n2*) and two representative mutant lamin–expressing cell lines (*LA1-LB1* and *LA1-LB3*) at 38°C (0 h) and after 8, 16, 24, and 48 h at 32°C. Low molecular weight DNA was isolated, resolved by electrophoresis on a 1% agarose gel, and visualized with ethidium bromide.

tation characteristic of apoptosis. Nuclear breakdown may be required to render the nucleases accessible to proteases or other agents that bring about their activation.

Kinetics of PARP and Lamin Cleavage In Vivo

In parallel with viability, cell extracts were prepared from a vector control cell line (Vh1-n2), two mutant lamin A– and lamin B–expressing cell lines (LA1-LB1 and LA2-LB3), and the E1B 19K–expressing cell line (19K1). Western blot analysis was used to detect PARP and lamin cleavage during p53-dependent apoptosis. PARP cleavage from a 116- to 85-kD fragment was observed 8 h after incubation at 32°C with all cell lines except the E1B 19K–expressing cell line, 19K1 (Fig. 9). Therefore, mutant lamin expression does not alter the activation of ICE-related PARP cysteine protease, as would be expected. No PARP cleavage was apparent in the E1B 19K–expressing cells at any time point (Fig. 9). Cleavage of endogenous lamin A/C was observed at the 8-h time point as indicated by the generation of the lamin A p47 and lamin C p37 polypeptides (Fig. 9). The kinetics of endogenous lamin cleavage in the mutant lamin–expressing cells was slightly delayed with less degradation products apparent at 8 h. At later times the degradation products were clearly distinguishable and identical to the controls (Fig. 9). Nuclear lamins are known to polymerize and assemble to form the nuclear lamina in association with the nuclear envelope (Nigg, 1992). It is possible that the overexpressed cleavage site lamin mutants copolymerize with the endogenous lamins and thereby protect the endogenous lamin A/C from proteolysis. The lamin A and lamin B cleavage site mutants, on the contrary, were completely resistant to proteolysis or degradation as seen in Western blots with anti-myc and -FLAG epitope antibodies (Fig. 9). Some nonspecific proteolysis of mutant lamin B was seen after 48 h of incubation at the permissive temperature when cell viability was very low. Actin serves as a control for protein loading (Fig. 9).

These results indicated that first, the attenuation of apoptosis observed upon mutant lamin expression (Fig. 7 *c*) was the result of events that occurred downstream of protease activation; secondly, cleavage of PARP proceeded independently of lamin cleavage; and finally, the cleavage-site lamin mutants were resistant to protease action in vivo, confirming that the site altered by mutagenesis was the site of lamin proteolysis.

Ultrastructural and Morphological Analysis of the Mutant Lamin–expressing Cells

Despite the delay in the onset of apoptosis, mutant lamin–expressing cells lost viability after 18 h at 32°C and showed gross morphological alterations indicative of apoptosis similar to the vector control cells. Ultrastructural analysis was performed to document the nuclear events occurring during apoptosis in the presence and absence of uncleavable lamins. Vh1-n1 cells at 38°C were ultrastructurally normal (Fig. 10 *a*) and no different in appearance from cell lines expressing mutant lamin A and B (LA1-LB1) at 38°C (data not shown). Higher magnification (20,000) showed an intact and well-defined lamina with an even distribution of nuclear pores (Fig. 10 *b*). The vector control cells examined after 24-h incubation at 32°C were morphologically apoptotic at the level of the light microscope when the majority of the cell population was detached and the viability was low (see Fig. 7 *c*). Electron micrographs showed these cells to have a hollow nucleus with condensed chromatin (Fig. 10 *c*), and the lamina was less apparent at the nuclear periphery, although the nuclear envelope appeared intact (Fig. 10 *d*) as has been observed previously (Wyllie, 1980). In contrast, >40% of the mutant lamin–expressing cells had a striking phenotype, whereby the lamina remained intact (Fig. 10 *f*) and the nu-

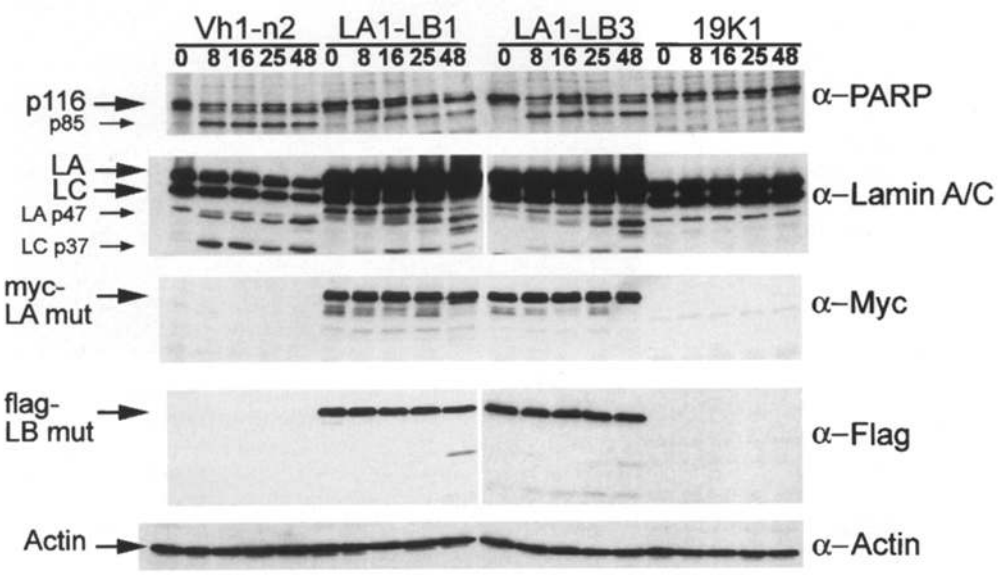

Figure 9. Cleavage-site mutants of lamins are not degraded in vivo during p53-dependent apoptosis. Western blot analysis of Vh1-n2, LA1-LB1, LA1-LB3, and 19K1 cells. Cell extracts were obtained in parallel with viability estimations (Fig. 7 *c*) at the restrictive temperature (0 h) and after incubating at the permissive temperature for 8, 16, 24, and 48 h. Blots were probed with antibodies specific for PARP (C-2-10), lamin A/C, the myc epitope tag to detect mutant lamin A, the FLAG epitope tag to detect mutant lamin B, and actin. The position of the cleavage product for PARP is indicated as p85, and for lamin A and C as LA p47 and LC p37, respectively. Actin served as a control for protein loading.

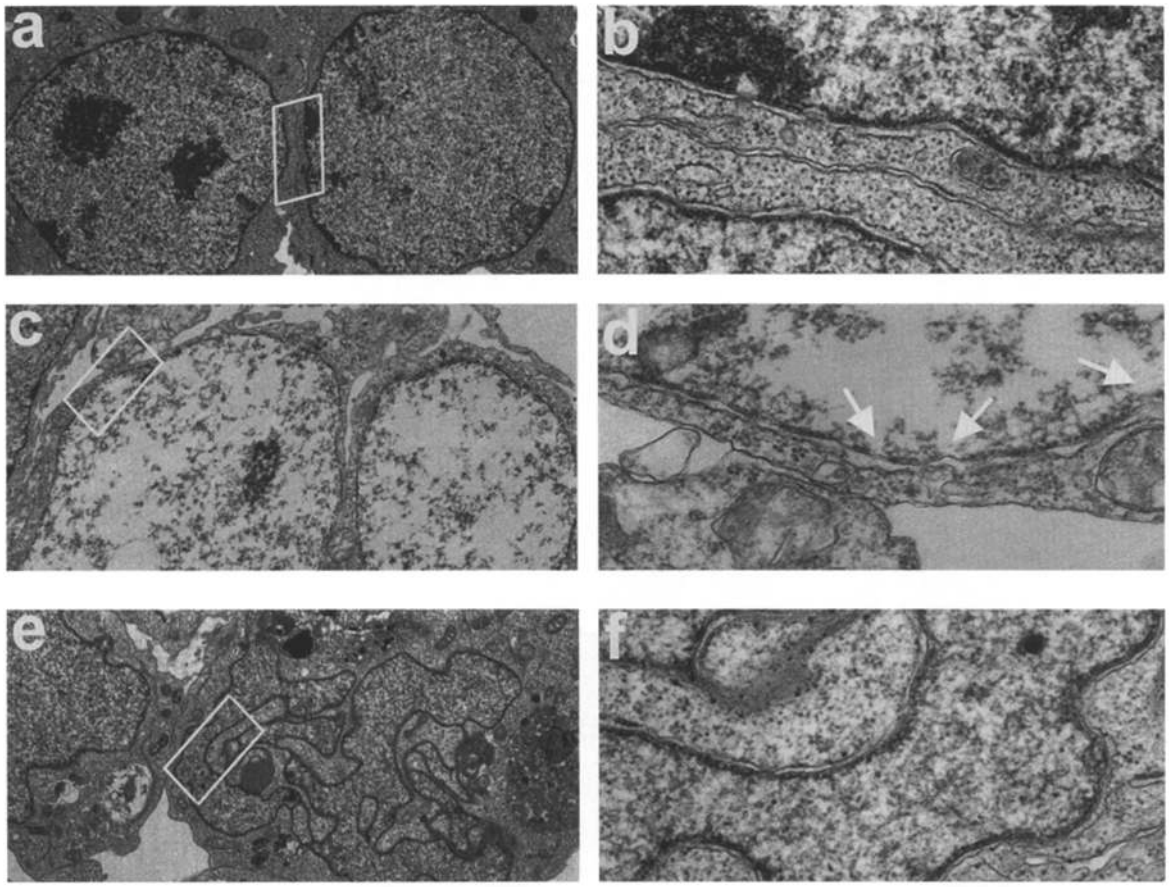

Figure 10. Ultrastructure of the mutant lamin–expressing cells. The mutant lamin–expressing cell line (LA1-LB1) was processed for EM after incubation at 32°C for 24 h (*e* and *f*). Control lines at 38°C (*a* and *b*) or after 24 h at 32°C (*c* and *d*) were also processed simultaneously. The exact region magnified is boxed in the lower magnification image. (*Arrows*) Regions of degrading lamina.

cleus involuted (Fig. 10 *e*). Higher magnification showed an electron-dense lamina still intact and underlying a convoluted nuclear envelope (Fig. 10 *f*).

Indirect immunofluorescence was performed on the mutant lamin A– and lamin B–expressing cells and the vector control cells to examine the morphology of the nucleus and the status of the mutant lamins as the cells were undergoing apoptosis. Staining with antibodies directed against the myc epitope to visualize mutant lamin A (Fig. 11) and with the FLAG epitope to visualize mutant lamin B (data not shown) revealed bright staining of the lamina as a result of the expression of the mutant proteins. The mutant lamin proteins localized to the nuclear envelope in a staining pattern that was indistinguishable from the endogenous lamins (Fig. 2). Hoechst dye staining to visualize DNA showed condensed chromatin along the periphery of the nucleus in apoptotic cells of the vector control cell line (Vh1-n1) (Fig. 11). On the contrary, the mutant lamin–expressing cells reflected the observations made from ultrastructural analysis. In >50% of the cells that had rounded up and appeared to be apoptotic, staining the DNA with Hoechst dye showed convoluted structures with DNA lining the nuclear periphery (Fig. 11). The mutant lamin stained brightly in these cells, indicating their resistance to proteolysis (Fig. 11). The DNA appeared to localize at the lamina, and the absence of any cells showing signs of classical chromatin condensation was striking. These observations confirm the morphology reported when lamin proteolysis was inhibited in vitro by TLCK (Lazebnik et al., 1995), where the chromatin formed a continuous rim around the periphery of the nucleus in cell-free extracts. However, the terminal morphology assessed by Hoechst dye staining of the floating cells at 28 h was invariant between the mutant lamin A– and lamin B–expressing cells and the corresponding controls. DNA staining clearly showed the formation of apoptotic bodies in both populations (Fig. 11). Thus, the formation of the late stage (terminal) phenotype of apoptotic cell death was unaltered by inhibiting lamin cleavage in vivo.

In summary, expression of the uncleavable mutants of lamins resistant to proteolysis in vivo delayed cell death and conferred altered morphology to the cells when they did undergo apoptosis. A protease-resistant lamina prevented the chromatin from condensing against the periphery of the nucleus and caused the convolution of the nucleus along the lamina carrying the nuclear envelope with it. This suggests a role for lamin proteolysis in bringing about some of the nuclear changes observed during apoptosis.

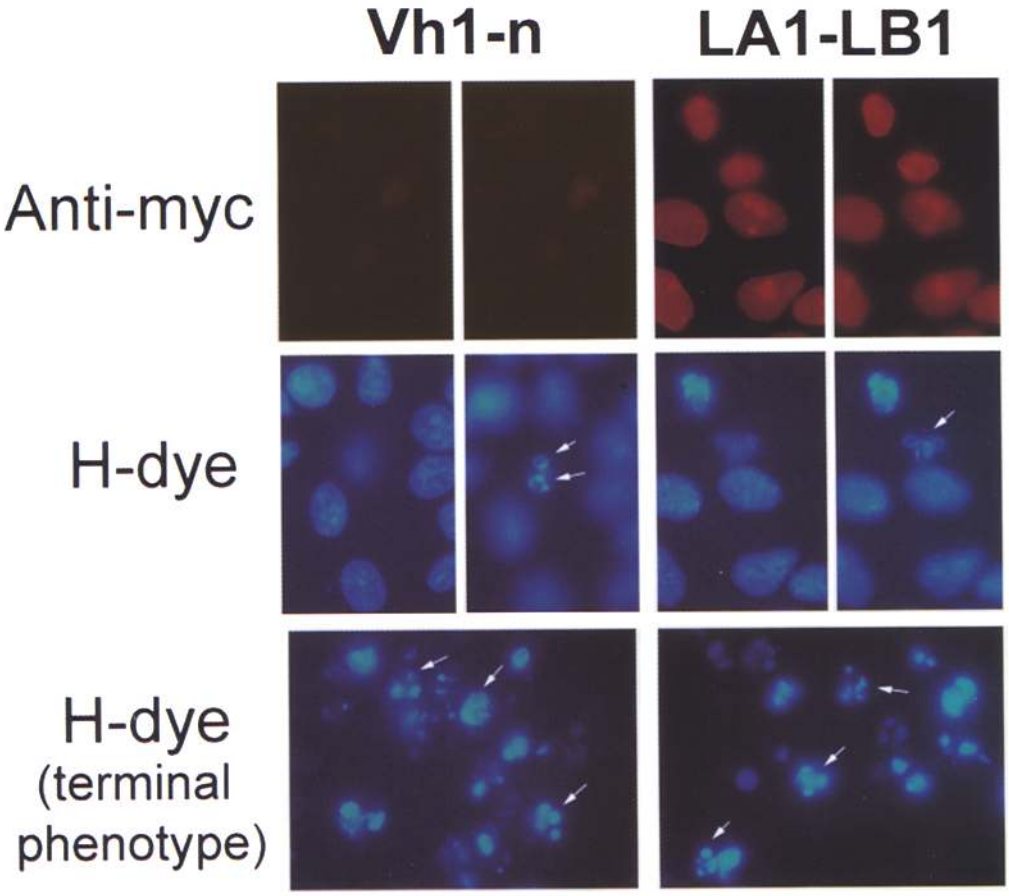

Figure 11. Morphology of the mutant lamin–expressing cells. The expression of mutant lamin A was visualized by immunofluorescence staining with anti-myc epitope antibodies after incubating the cells at 32°C for 24 h. Vector control lines were processed in parallel. Hoechst dye staining was also done to visualize DNA. Photographs are in two planes of focus with the apoptotic cells indicated by arrows. (*Bottom panel*) Terminal phenotype as seen in the floating cells by in situ staining with Hoechst dye. (*Arrows*) Representative cells with distinct apoptotic bodies.

Discussion

Apoptosis induced by adenovirus E1A displays all the classical morphological events of apoptosis (Rao et al., 1992; White et al., 1992; Wyllie, 1980). Furthermore, the E1B 19K protein is the adenoviral equivalent of the mammalian protooncogene product Bcl-2 and inhibits apoptosis to maximize viral yield (Chiou et al., 1994*b*) and to promote transformation (Rao et al., 1992). This argues for conserved genetic elements in apoptosis present in varied systems ranging from viruses to mammals. It is therefore conceivable that the biochemical pathways and mechanisms of the process are also conserved. In fact, induction of the Bcl-2 antagonist, Bax, is a biochemical event downstream of p53 that promotes E1A-induced apoptosis (Han et al., 1996*a*). Activation of the ICE family of cysteine proteases is another biochemical event that occurs during apoptosis that has been preserved through evolution (Martin and Green, 1995; Whyte and Evan, 1995; Yuan et al., 1993). Processing of CPP32, a representative member of the ICE family, has been observed during p53-dependent apoptosis and requires a transcriptionally competent p53 (Sabbatini, P., J. Han, S.-K. Chiou, D.W. Nicholson, and E. White, manuscript in preparation). Activation of the lamin protease and the site-specific cleavage of lamins observed in this study is further testimony to the activation of ICE-related cysteine proteases downstream of p53. ICE-related protease activation could be a direct or indirect consequence of Bax induction. The E1B 19K protein functions as an apoptosis inhibitor in BRK cells by physically complexing with the death-inducing proteins Bax and Nbk/Bik (Han et al., 1996*a*, *b*). Absence of any lamin degradation or activation of lamin proteases in E1B 19K–expressing cells places the 19K protein upstream of protease activation in the pathway. Activation of CPP32 and cleavage of PARP is observed when p53 null cells are infected with 19K$^-$ viruses expressing only E1A (Boulakia et al., 1996). Coexpression of E1B 19K can prevent activation of CPP32 and cleavage of PARP in both p53-dependent and -independent situations (Boulakia et al., 1996; Sabbatini, P., J. Han, S.-K. Chiou, D.W. Nicholson, and E. White, manuscript in preparation). Bax and Nbk may represent the p53-dependent and -independent upstream elements, respectively, for bringing about protease activation. The E1B 19K protein is able to effectively inhibit both of these cytotoxic proteins by interactions via the BH3 domain (Boyd et al., 1995; Han et al., 1996*a*,*b*). CPP32 does not cleave lamins in vitro, and activation of parallel proteinase pathways has been proposed (Lazebnik et al., 1995). Therefore, it appears that at least two proteases are activated either in parallel or in tandem during E1A-induced apoptosis. This suggests that the E1B 19K protein potently inhibits apoptosis by functioning far upstream to prevent the biochemical process leading to the activation of multiple cysteine proteases.

The site of lamin cleavage was mapped to a conserved aspartate residue at position 230 and has been confirmed with mutational analysis both in vitro and in vivo. This lamin cleavage site was mapped to the same aspartate residue independently by different methods (Takahashi et al.,

1996). The cleavage site lies in the center of the α-helical rod domain of all three types of lamins. The α-helical rod domain is important for dimerization and higher order assembly of the lamina (McKeon, 1991). The presence of specific chromatin binding sites in this domain has also been demonstrated (Glass et al., 1993). Cleavage at this site may represent an effective mechanism of breaking down the lamina and releasing the chromatin at specific sites to assist condensation and packaging into apoptotic bodies. A second cleavage site at position 446 in the context of a consensus cleavage site is not recognized by the lamin protease. Also, lamin A is specifically cleaved by the ICE-like proteases Mch-2α but not CPP32 (Orth et al., 1996; Takahashi et al., 1996). This type of specificity between enzymes, substrates, and the cleavage site could come from availability of the site for proteolysis in the three-dimensional structure of the protein and/or the context of the cleavage site in relation to the surrounding amino acid sequence.

PARP, as a substrate, has become an indicator for cysteine proteases activated during apoptosis (Lazebnik et al., 1994). The relevance of PARP as a substrate in vivo appears limited, as knocking out the gene results in specific defects in ribosylation with otherwise normal mice (Wang et al., 1995). Lamins may be more relevant in vivo as a result of their role in maintenance of the structural elements that hold the nucleus together. Lamin degradation and breakdown has been reported in different cell types and in response to different apoptosis-inducing stimuli (Neamati et al., 1995; Oberhammer et al., 1994; Ucker et al., 1992). Furthermore, the attenuation of cell death we have observed upon expressing uncleavable lamins implicates the lamins as key substrates targeted for degradation relatively early in the apoptotic process. The degradation of lamin B1 has been reported to precede DNA fragmentation in thymocytes undergoing apoptosis (Neamati et al., 1995). Inhibition of lamin proteinases does not prevent internucleosomal DNA cleavage in the cell-free system with HeLa nuclei (Lazebnik et al., 1995). In vivo we have observed DNA fragmentation to be delayed in the mutant lamin–expressing cells, indicating that activation of the nucleases functional during apoptosis is dependent on breakdown of the lamina and overall nuclear disintegration. The in vitro results reflect an end point analysis when the nucleases are active (Lazebnik et al., 1995), as we have observed. However, kinetic analysis of DNA fragmentation in the mutant lamin–expressing cells indicated a delay in the activation of nucleases during apoptosis. Obviously, preventing lamin cleavage is not sufficient to inhibit apoptosis, as subsequent events take over and bring about cell death. The attenuation of apoptosis observed here is significant in establishing the sequence of events downstream of protease activation. Inhibiting lamin cleavage prevents loss of cell viability until perhaps proteolytic attack of other substrates promotes nuclear degradation and the cell succumbs.

Clues to the role of lamin proteolysis in apoptosis have come from the ultrastructure and morphological analysis of these cells expressing uncleavable mutant lamins. Although the cells expressing mutant lamins lose viability, their lamina remains intact and assumes a convoluted appearance (Fig. 12). The shrinkage of nuclei seen in control

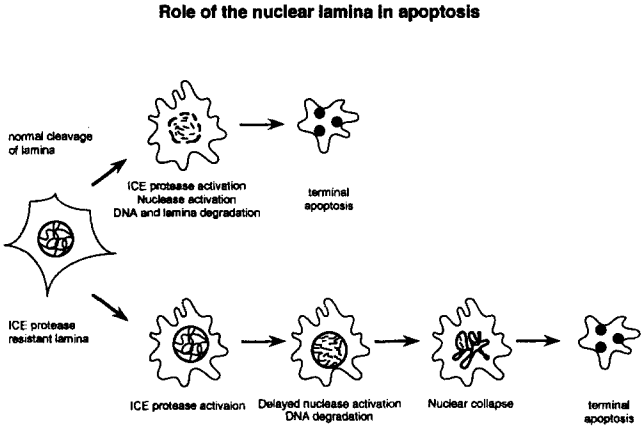

Figure 12. Model for the possible role of the lamina during apoptosis. Schematic model to explain the observations made, indicating a role for lamin degradation in the execution of cell death processes.

cells undergoing apoptosis is markedly absent in the mutant lamin–expressing cells. Instead, collapse of the nuclear envelope with the lamina is observed in the absence of chromatin condensation (Fig. 12). Lazebnik et al. have reported a similar inability of the chromatin to condense upon inhibiting lamin proteases in vitro (Lazebnik et al., 1995). The reflection of this phenomenon in vivo suggests a role for lamin proteolysis in the nuclear events of apoptosis.

There are three, not necessarily mutually exclusive, models to account for a role of lamin cleavage in apoptosis that are consistent with our observations. First, inhibiting lamin proteolysis may prevent detachment of DNA at the sites where it contacts the lamina, since lamins serve to anchor and to organize chromatin at the nuclear periphery. This would result in the inability of the chromatin to condense into discrete packages; instead, the DNA would collapse against the periphery of the nucleus. Hollowing of the nucleus, in addition to the stress created by the chromatin still attached to the lamins, may cause the lamina to involute along with the nuclear membranes. Second, an uncleavable lamina may prevent the shrinkage of nuclei imposing an additional restriction. Thus, the proteolysis of lamins allows for condensation of the chromatin into aggregates for rapid packaging into membrane-bound apoptotic bodies. Third, lamin breakdown may facilitate nuclear breakdown by opening up the nucleus and permitting degradation of other nuclear substrates as well as rendering the nucleases accessible to activation by cytoplasmic factors. In conclusion, the lamins represent a key substrate for the proteases activated during apoptosis whose degradation facilitates the nuclear events of apoptosis.

We thank Mr. Raj Patel for assistance with the electron microscopy.

This work has been supported by a grant from the National Institutes of Health (CA53370) to E. White.

Received for publication 26 July 1996 and in revised form 14 September 1996.

References

Boldin, M.P., T.M. Goncharov, Y.V. Goltsev, and D. Wallach. 1996. Involvement of MACH, a novel MORT1/FADD-interacting protease, in Fas/APO-1-

and TNF receptor-induced cell death. *Cell.* 85:803–815.

Boulakia, C.A., G. Chen, F.W.H. Ng, J.G. Teodoro, P.E. Branton, D.W. Nicholson, G.G. Poirier, and G.C. Shore. 1996. Bcl-2 and adenovirus E1B 19 kDA protein prevent E1A-induced processing of CPP32 and cleavage of poly(ADP-ribose) polymerase. *Oncogene.* 12:529–535.

Boyd, J.M., G.J. Gallo, B. Elangovan, A.B. Houghton, S. Malstrom, B.J. Avery, R.G. Ebb, T. Subramanian, T. Chittenden, R.J. Lutz, and G. Chinnadurai. 1995. Bik1, a novel death-inducing protein shares a distinct sequence motif with Bcl-2 family proteins and interacts with viral and cellular survival-promoting proteins. *Oncogene.* 11:1921–1928.

Chinnaiyan, A.M., K. Orth, K. O'Rourke, H. Duan, G.G. Poirier, and V.M. Dixit. 1996. Molecular ordering of the cell death pathway. *J. Biol. Chem.* 271:4573–4576.

Chiou, S.-K., L. Rao, and E. White. 1994*a*. Bcl-2 blocks p53-dependent apoptosis. *Mol. Cell. Biol.* 14:2556–2563.

Chiou, S.-K., C.C. Tseng, L. Rao, and E. White. 1994*b*. Functional complementation of the adenovirus E1B 19K protein with Bcl-2 in the inhibition of apoptosis in infected cells. *J. Virol.* 68:6553–6566.

Debbas, M., and E. White. 1993. Wild-type p53 mediates apoptosis by E1A which is inhibited by E1B. *Genes & Dev.* 7:546–554.

Duan, H., A.M. Chinnaiyan, P.L. Hudson, J.P. Wing, W. He, and V.M. Dixit. 1996. ICE-LAP3, a novel mammalian homologue of the *Caenorhabditis elegans* cell death protein Ced-3 is activated during Fas- and tumor necrosis factor-induced apoptosis. *J. Biol. Chem.* 2713:1621–1625.

Earnshaw, W.C. 1995. Nuclear changes in apoptosis. *Curr. Opin. Cell Biol.* 7: 337–343.

Ellis, H., and H.R. Horvitz. 1986. Genetic control of programmed cell death in the nematode *C. elegans. Cell.* 44:817–829.

Ellis, H., J.-Y. Yuan, and H.R. Horvitz. 1991. Mechanisms and functions of cell death. *Annu. Rev. Cell Biol.* 7:663–698.

Faucheu, C., A. Diu, A.W.E. Chan, A.-M. Blanchet, C. Miossec, F. Herve, V. Collard-Dutilleul, Y. Gu, R.A. Aldape, J.A. Lippke, et al. 1995. A novel human protease similar to the interleukin-1β converting enzyme induces apoptosis in transfected cells. *EMBO (Eur. Mol. Biol. Organ.) J.* 14:1914–1922.

Fernandes-Alnemri, T., G. Litwack, and E. Alnemri. 1994. CPP32, a novel human apoptotic protein with homology to *Caenorhabditis elegans* cell death protein Ced-3 and mammalian interleukin-1β-converting enzyme. *J. Biol. Chem.* 269:30761–30764.

Fernandes-Alnemri, T., G. Litwack, and E.S. Alnemri. 1995*a*. *Mch2*, a new member of the apoptotic *Ced-3/ICE* cysteine protease gene family. *Cancer Res.* 55:2737–2742.

Fernandes-Alnemri, T., A. Takahashi, R. Armstrong, J. Krebs, L. Fritz, K.J. Tomaselli, L. Wang, Z. Yu, C.M. Croce, G. Salveson, et al. 1995*b*. Mch3, a novel human apoptotic cysteine protease highly related to CPP32. *Cancer Res.* 55:6045–6052.

Fraser, A., and G. Evan. 1996. A license to kill. *Cell.* 85:781–784.

Glass, C.A., J.R. Glass, H. Taniura, K.W. Hasel, J. Blevitt, and L. Gerace. 1993. The α-helical rod domain of human lamins A and C contains a chromatin binding site. *EMBO (Eur. Mol. Biol. Organ.) J.* 12:4413–4424.

Han, J., P. Sabbatini, D. Perez, L. Rao, D. Modha, and E. White. 1996*a*. The E1B 19K protein functions as an apoptosis inhibitor by interacting with and inhibiting the p53-inducible and death-promoting Bax protein. *Genes & Dev.* 10:461–477.

Han, J., P. Sabbatini, and E. White. 1996*b*. Induction of apoptosis by the E1B 19K binding protein, Nbk. *Mol. Cell Biol.* 16:5857–5864.

Heald, R., and F. McKeon. 1990. Mutations of phosphorylation sites in lamin A that prevent nuclear lamina disassembly in mitosis. *Cell.* 61:579–589.

Hirt, B. 1967. Selective extraction of polyoma DNA from infected mouse cultures. *J. Mol. Biol.* 26:365–369.

Kamens, J., M. Paskind, M. Huguinin, R.V. Talanian, H. Allen, D. Banach, N. Bump, M. Hackett, C.G. Johnston, P. Li, J.A. Mankovitch, M. Terranova, and T. Ghayur. 1995. Identification and characteriation of Ich-2, a novel member of the interleukin-1β-converting enzyme family of cysteine proteases. *J. Biol. Chem.* 270:15250–15256.

Kaufmann, S.H. 1989. Induction of endonucleolytic DNA cleavage in human acute myelogenous leukemia cells by etoposide, camptothectin, and other cytotoxic anticancer drugs: a cautionary note. *Cancer Res.* 49:5870–5878.

Kuida, K., J.A. Lippke, G. Ku, M.W. Harding, D.J. Livingston, M.S.-S. Su, and R.A. Flavell. 1995. Altered cytokine export and apoptosis in mice deficient in interleukin-1β converting enzyme. *Science (Wash. DC).* 267:2000–2003.

Kumar, S., M. Kinoshita, M. Noda, N.G. Copeland, and N.A. Jenkins. 1994. Induction of apoptosis by the mouse *Nedd2* gene, which encodes a protein similar to the product of the *Caenorhabditis elegans* cell death gene *ced-3* and the mammalian IL-1β-converting enzyme. *Genes & Dev.* 8:1613–1626.

Lazebnik, Y.A., S.H. Kaufmann, S. Desnoyers, G.G. Poirier, and W.C. Earnshaw. 1994. Cleavage of poly(ADP-ribose) polymerase by a proteinase with properties like ICE. *Nature (Lond.).* 371:346–347.

Lazebnik, Y., A. Takahashi, R. Moir, R. Goldman, G. Poirier, S. Kaufmann, and W. Earnshaw. 1995. Studies of the lamin proteinase reveal multiple parallel biochemical pathways during apoptotic execution. *Proc. Natl. Acad. Sci. USA.* 92:9042–9046.

Li, P., A. Hamish, S. Banejee, S. Franklin, L. Herzog, C. Johnston, J. McDowell, M. Paskind, L. Rodman, J. Salfeld, et al. 1995. Mice deficient in IL-1β-converting enzyme are defective in production of mature IL-1β and resistant to endotoxic shock. *Cell.* 80:401–411.

Martin, J.S., and R.D. Green. 1995. Protease activation during apoptosis: death by a thousand cuts? *Cell.* 82:349–352.

Martinez, J., I. Georgoff, J. Martinez, and A.J. Levine. 1991. Cellular localization and cell cycle regulation by a temperature-sensitive p53 protein. *Genes & Dev.* 5:151–159.

McKeon, F. 1991. Nuclear lamin proteins: domains required for nuclear targeting, assembly, and cell-cycle-regulated dynamics. *Curr. Opin. Cell Biol.* 3:82–86.

McKeon, F.D., M.W. Kirschner, and D. Caput. 1988. Homolgies in both primary and secondary structure between nuclear envelope and intermediate filament proteins. *Nature (Lond.).* 319:463–468.

Michalovitz, D., O. Halevy, and M. Oren. 1990. Conditional inhibition of transformation and of cell proliferation by a temperature-sensitive mutant of p53. *Cell.* 62:671–681.

Miura, M., H. Zhu, R. Rotello, E.A. Hartwieg, and J. Yuan. 1993. Induction of apoptosis in fibroblasts by IL-1β-converting enzyme, a mammalian homolog of the *C. elegans* cell death gene *ced-3. Cell.* 75:653–660.

Moran, E. 1993. DNA tumor virus transforming proteins and the cell cycle. *Curr. Opin. Genet. Dev.* 3:63–70.

Munday, N.A., J.P. Vaillancourt, A. Ali, F.J. Casano, D.K. Miller, S.M. Molineaux, T.-T. Yamin, V.L. Yu, and D.W. Nicholson. 1995. Molecular cloning and pro-apoptotic activity of ICErel-II and ICErel-III, members of the ICE/CED-3 family of cysteine proteases. *J. Biol. Chem.* 270:15870–15876.

Muzio, M., A.M. Chinnaiyan, F.C. Kischkel, K. O'Rourke, A. Shevchenko, J. Ni, C. Scaffidi, J.D. Bretz, M. Zhang, R. Gentz, et al. 1996. FLICE, A novel FADD-homologous ICE/CED-3-like protease, is recruited to the CD95 (Fas/APO-1) death-inducing signaling complex. *Cell.* 85:817–827.

Neamati, N., A. Fernandez, S. Wright, J. Kiefer, and D.J. McConkey. 1995. Degradation of Lamin B1 precedes oligonucleosomal DNA fragmentation in apoptotic thymocytes and isolated thymocyte nuclei. *J. Immunol.* 154: 3788–3795.

Nicholson, D.W., A. Ali, N.A. Thornberry, J.P. Vaillancourt, C.K. Ding, M. Gallant, Y. Gareau, P.R. Griffin, M. Labelle, Y.A. Lazebnik, et al. 1995. Identification and inhibition of the ICE/CED-3 protease necessary for mammalian apoptosis. *Nature (Lond.).* 376:37–43.

Nigg, E.A. 1992. Assembly and cell cycle dynamics of the nuclear lamina. *Semin. Cell Biol.* 3:245–253.

Oberhammer, F.A., K. Hochegger, G. Froschl, R. Tiefenbacher, and M. Pavelka. 1994. Chromatin condensation during apoptosis is accompanied by degradation of lamin A+B, without enhanced activation of cdc2 kinase. *J. Cell Biol.* 126:827–837.

Orth, K., M.A. Chinnaiyan, M. Garg, J.C. Froelich, and M.V. Dixit. 1996. The CED-3/ICE like protease Mch-2 is activated during apoptosis and cleaves the death substrate lamin A. *J. Biol. Chem.* 271:16720–16724.

Peter, M., J. Nakagawa, M. Doree, C.J. Labbe, and E.A. Nigg. 1990. In vitro disassembly of the nuclear lamina and M-phase specific phosphorylation of lamins by cdc-2. *Cell.* 61:591–602.

Pollard, M.J., K.L.E. Chan, J.B. Grant, F.K. Sullivan, M.E. Tan, and A.E. Glass. 1990. In vitro posttranslational modification of lamin B cloned from a human T-cell line. *Mol. Cell Biol.* 10:2164–2175.

Raff, M.C. 1992. Social controls on cell survival and cell death. *Nature (Lond.).* 356:398–400.

Rao, L., M. Debbas, P. Sabbatini, D. Hockenberry, S. Korsmeyer, and E. White. 1992. The adenovirus E1A proteins induce apoptosis which is inhibited by the E1B 19K and Bcl-2 proteins. *Proc. Natl. Acad. Sci. USA.* 89:7742–7746.

Sabbatini, P., S.-K. Chiou, L. Rao, and E. White. 1995*a*. Modulation of p53-mediated transcription and apoptosis by the adenovirus E1B 19K protein. *Mol. Cell. Biol.* 15:1060–1070.

Sabbatini, P., J. Lin, A.J. Levine, and E. White. 1995*b*. Essential role for p53-mediated transcription in apoptosis but not growth suppression. *Genes & Dev.* 9:2184–2192.

Takahashi, A., E.S. Alnemri, Y.A. Lazebnik, T. Fernandes-Alnemri, G. Litwack, R.D. Moir, R.D. Goldman, G.G. Poirier, S.H. Kaufmann, and W.C. Earnshaw. 1996. Cleavage of lamin A by Mch2α but not CPP32: multiple ICE-related proteases with distinct substrate recognition properties are active in apoptosis. *Proc. Natl. Acad. Sci. USA.* 93:8395–8400.

Tewari, M., L.T. Quan, K. O'Rourke, S. Desnoyers, Z. Zeng, D.R. Beidler, G. Poirier, G.S. Salvesen, and V.M. Dixit. 1995. Yama/CPP32β, a mammalian homolog of CED-3, is a CrmA-inhibitable protease that cleaves the death substrate poly(ADP-ribose) polymerase. *Cell.* 81:801–809.

Thornberry, N.A., H.G. Bull, J.R. Calaycay, K.T. Chapman, A.D. Howard, M.J. Kostura, D.K. Miller, S.M. Molineaux, J.R. Weidner, and J. Aunins. 1992. A novel heterodimeric cysteine protease is required for interleukin-1β processing in monocytes. *Nature (Lond.).* 356:768–774.

Ucker, D.S., J. Meyers, and P.S. Obermiller. 1992. Activation driven cell death: quantative differences alone distinguish stimuli triggering nontransformed T cell proliferation or death. *J. Immunol.* 149:1583–1592.

Wang, L., M. Miura, L. Bergeron, H. Zhu, and J. Yuan. 1994. *Ich-1*, an *ICE/ced-3*-related gene, encodes both positive and negative regulators of programmed cell death. *Cell.* 78:739–750.

Wang, Z.-Q., B. Auer, L. Stingl, H. Berghammer, D. Haidacher, M. Schweiger, and E.F. Wagner. 1995. Mice lacking ADPRT and poly(ADP-ribosyl)ation develop normally but are susceptible to skin disease. *Genes & Dev.* 9:509–520.

Ward, E.G., and W.M. Kirschner. 1990. Identification of cell cycle-regulated phosohorylation sites on nuclear lamin C. *Cell.* 61:561–577.

White, E. 1995. Regulation of p53-dependent apoptosis by E1A and E1B. *In* Current Topics in Microbiology and Immunology: The Molecular Repertoire of Adenovirus. W. Doerfler, editor. Springer Verlag, Berlin/Heidelberg. 199:33–58.

White, E. 1996. Life, death, and the pursuit of apoptosis. *Genes & Dev.* 10:1–15.

White, E., and R. Cipriani. 1989. Specific disruption of intermediate filaments and the nuclear lamina by the 19-kDa product of the adenovirus E1B oncogene. *Proc. Natl. Acad. Sci. USA.* 86:9886–9890.

White, E., T. Grodzicker, and B.W. Stillman. 1984. Mutations in the gene encoding the adenovirus E1B 19K tumor antigen cause degradation of chromosomal DNA. *J. Virol.* 52:410–419.

White, E., R. Cipriani, P. Sabbatini, and A. Denton. 1991. The adenovirus E1B 19-kilodalton protein overcomes the cytotoxicity of E1A proteins. *J. Virol.* 65:2968–2978.

White, E., P. Sabbatini, M. Debbas, W.S.M. Wold, D.I. Kusher, and L. Gooding. 1992. The 19-kilodalton adenovirus E1B transforming protein inhibits programmed cell death and prevents cytolysis by tumor necrosis factor α. *Mol. Cell. Biol.* 12:2570–2580.

White, E., L. Rao, S.-K. Chiou, C.-C. Tseng, P. Sabbatini, M. Gonzalez, and P. Verwaerde. 1994. Regulation of apoptosis by the transforming gene products of adenovirus. *In* Apoptosis. E. Mihich and R.T. Shimke, editors. Plenum Press, New York 47–62.

Whyte, M., and G. Evan. 1995. The last cut is the deepest. *Nature (Lond.).* 376: 17–18.

Wyllie, A.H. 1980. Cell death: the significance of apoptosis. *Int. Rev. Cytol.* 68: 251–306.

Yuan, J., S. Shaham, S. Ledoux, H.M. Ellis, and H.R. Horvitz. 1993. The *C. elegans* cell death gene ced-3 encodes a protein similar to mammalian interleukin-1β-converting enzyme. *Cell.* 75:641–652.

Zheng, H., D. Fletcher, W. Kozak, M. Jiang, K. Hofmann, C.A. Conn, D. Soszynski, C. Grablec, M. Trumbauer, A. Shaw, et al. 1995. Resistance to fever induction and impaired acute phase response in interleukin-1β deficient mice. *Immunity.* 3:9–19.